Advances in Materials Physics and Chemistry, **2013, 3, 58-61**
http://dx.doi.org/10.4236/ampc.2013.31009 Published Online March 2013 (http://www.scirp.org/journal/ampc)

Thickness Dependence of Dielectric Characteristics of $SrTiO_3$ Thin Films on $MgAl_2O_4$ Substrates

Ryuhei Kinjo, Iwao Kawayama, Hironaru Murakami, Masayoshi Tonouchi
Institute of Laser Engineering, Osaka University, Osaka, Japan
Email: tonouchi@ile.osaka-u.ac.jp

Received December 27, 2012; revised January 28, 2013; accepted February 7, 2013

ABSTRACT

$SrTiO_3$ (STO) thin films of different thicknesses were deposited on $MgAl_2O_4$ (MAO) substrates to investigate the in-plane strain effect on the soft-mode frequency of the STO films. X-ray reciprocal space mapping (X-RSM) results indicate that there was no relaxation of the in-plane lattice strain of the STO films on MAO. Shifts in the soft-mode frequencies with a decrease in the film thickness were observed using terahertz time-domain spectroscopy (THz-TDS). However, despite the larger lattice mismatch between STO and MAO than that between STO and $DyScO_3$ (DSO), the shifts in the soft-mode frequencies of the STO films on MAO were smaller than those on DSO. The results indicate that the soft-mode frequencies of the STO films on MAO are affected by the *c*-axis (out-of-plane) lengths.

Keywords: Strontium Titanate; Ferroelectric; Soft Mode; Thin Film; Strain Effect

1. Introduction

Strontium titanate (STO) is a transition metal oxide that has a perovskite structure. Pure bulk single-crystal STO is a known quantum paraelectric that does not undergo a ferroelectric phase transition even at temperatures close to 0 K, and its permittivity is as high as 10^4 at low temperatures [1]. From theoretical predictions, lattice strain in STO changes the phase transition temperature drastically and induces ferroelectricity [2], and, in fact, Haeni *et al.* [3] have reported room-temperature ferro-electricity in a strained STO thin film deposited on a $DyScO_3$ (DSO) substrate. Since that report, various studies of strained STO thin films have been conducted, e.g., thermodynamic analysis of anisotropically strained films [4] and electric and spectrometric measurements [5-9]. However, there have only been a few reports concerning the ferroelectric and dielectric properties of STO thin films induced by large in-plane strain. In our previous study, we observed the dielectric dispersion of STO thin films on $MgAl_2O_4$ (MAO) substrates with a lattice mismatch of +3.39%, which is much larger than the lattice mismatch of +0.99% between STO and DSO. The temperature dependence of the dielectric dispersion of a 360 nm thick STO film on MAO in the terahertz region showed signs of a ferroelectric phase transition at around 170 K, much lower than that expected from the lattice mismatch [10]. We concluded, therefore, that the strain in the STO thin film on MAO used in that experiment was somewhat relaxed, and sufficient strain required for the generation of ferroelectricity at room temperature was not induced in the film. However, further experimental study is necessary to reveal the strain effects in STO thin films on MAO substrates.

In this study, we measured the thickness dependence of the dielectric dispersions of STO thin films on MAO substrates using terahertz time-domain spectroscopy (THz-TDS), and the in-plane lattice constants of the films were determined using X-ray reciprocal space maping (X-RSM). Moreover, we measured the dielectric dispersions and lattice constants of STO films on $(La_{0.3}Sr_{0.7})(AL_{0.65}Ta_{0.35})O_3$ (LSAT) and DSO substrates for comparison to elucidate the lattice strain effect on the dielectric characteristics.

2. Experimental Methods

We deposited STO films with thicknesses of 60, 120, 360, and 650 nm on MAO substrates by pulsed laser deposition. STO thin films were also deposited on LSAT and DSO substrates to compare the relationship between the in-plane strain induced by the lattice mismatch and the extension or contraction of the *c*-axis. A θ - 2θ X-ray diffraction (XRD) method was used to evaluate the crystalline quality and determine the *c*-axis lengths of the films. Only (00*l*) diffraction peaks were observed in the θ - 2θ XRD patterns, which indicated that the films were good *c*-axis orientation films. Additionally, X-RSM using a Rigaku SmartLab diffractometer was used for the 360 nm thick STO film on MAO to observe the inplane

lattice constant. The dielectric dispersions of the STO films were observed using a broadband THz-TDS system with a 4-dimethylamino-*N*-methyl-4-stilbazolium tosylate (DAST) crystal as the terahertz emitter. DAST is an organic nonlinear optical crystal that can emit broad- band terahertz waves by pulsed laser irradiation except at around 1.1 THz where a large absorption peak of the DAST exists. Details of the experimental setup have been reported elsewhere [11].

3. Results and Discussion

Table 1 shows the lattice mismatch between each substrate and the STO single crystal, thicknesses, and *c*-axis lengths of the STO films on the MAO, LSAT, and DSO substrates. The *c*-axis lengths of the STO films on MAO were 0.3895, 0.3899, and 0.3900 nm for the 60 nm, 120 nm, and 360 nm thick films, respectively. The *c*-axis length of the 650 nm thick film, 0.3900 nm, is equal to that of the 360 nm thick film. The *c*-axis lengths of the STO films on the LSAT and DSO substrates were 0.3936 nm and 0.3885 nm, respectively. The *c*-axis length of the STO film on LSAT is longer than that of a bulk STO single crystal owing to in-plane compressive strain, while that on DSO was compressed owing to in-plane tensile strain. For the STO films on MAO, the *c*-axis was compressed because of in-plane tensile strain but did not change by an amount as large as that in the case of the STO films on DSO. For films on MAO thinner than 360 nm, the *c*-axis lengthens slightly with an increase in the film thickness. However, there was no extension of the *c*-axis for films on MAO thicker than 360 nm.

Figure 1 shows the results of the X-RSM measurement around the (112) reflection of the 360 nm thick STO film on MAO. The vertical axis $Q_{\perp}$(1/Å) corresponds to the *c*-axis direction, and the horizontal axis $Q_{\parallel}$(1/Å) correspond to the *a*-axis (in-plane) of the STO film. The origin in $Q_{\parallel}$-axis is set at the (224) reflection of MAO. The two sharp peaks in the lower part of **Figure 1** arise from the (224) reflection of MAO and are attributed to the Cu Kα_1 and Kα_2 lines of the X-ray source. The peaks are separated due to the high crystalline quality of the MAO substrate, and the tilting of the peaks indicates that the MAO substrate has some variation in its lattice constants. The broad single peak in the upper part of **Figure 1** is the (112) reflection of the STO thin film. There is no separation of the Cu Kα_1 and Kα_2 lines, and the broadness indicates the mosaicity of the film. Although the (112) reflection of the STO film was broader than that of the MAO (224), they have almost the same $Q_{\parallel}$ value, and no diffraction signals were seen around the calculated (112) reflection position of bulk STO (indicated by the cross mark). These results demonstrate that the in-plane lattice constant of the STO thin film on MAO corresponded to that of the MAO substrate and that the STO films were fully stained without any relaxation.

Figure 2 shows the dielectric dispersions of the four STO thin films on MAO measured by THz-TDS at room temperature. Note that the irregular dielectric dispersion observed at around 1.1 THz is not an intrinsic characteristic of the films.

We fitted the data to both the real and imaginary parts of the dielectric dispersion using a classical damping-oscillator dispersion model given by the following Equation:

$$\varepsilon(\omega) = \varepsilon_{\infty} + \frac{\Delta\varepsilon\omega_{\mathrm{TO1}}^2}{\omega_{\mathrm{TO1}}^2 - \omega^2 - i\gamma_{\mathrm{TO1}}\omega} \quad (1)$$

where ε_{∞} is the high-frequency dielectric constant, $\Delta\varepsilon$ is the dielectric strength, ω_{TO1} is the soft-mode frequency, and γ_{TO1} is the damping constant. The dashed lines in

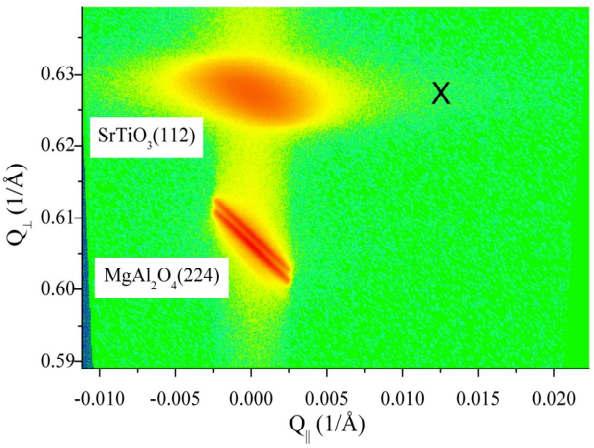

Figure 1. X-ray reciprocal space mapping around the asymmetric (112) Bragg reflection of the 360 nm thick $SrTiO_3$ thin film on a $MgAl_2O_4$ substrate.

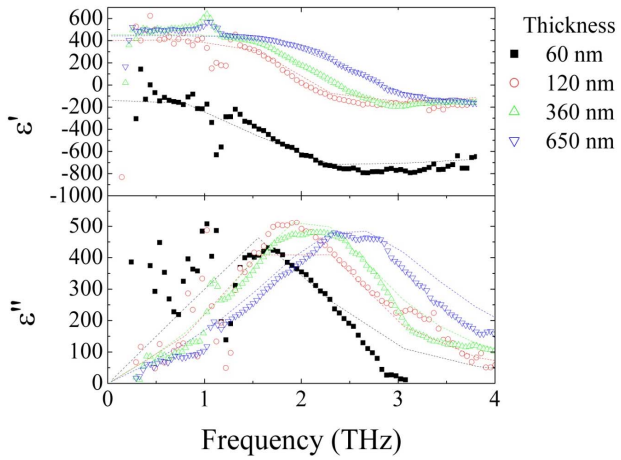

Figure 2. Thickness dependence of the dielectric dispersion of the $SrTiO_3$ thin films on $MgAl_2O_4$ substrates.

Figure 2 are the results of the fitting. The reported soft-mode frequencies of STO single crystals are around 2.7 - 3.0 THz [12-14], but the soft-mode frequency of the 650 nm thick STO thin film on MAO is 2.6 THz, which is a slightly lower frequency. The soft-mode frequency shifted to a lower frequency with a decrease in the film thickness. In the case of the 60 nm thick film, the dielectric dispersion varied widely below 1.1 THz, and the real part of the dielectric constant was noticeably smaller than the other films. This is due to the low signal-noise ratio of the 60 nm thick film, therefore the absolute value was not accurate, but it did not affect the estimation of soft-mode frequency.

Figure 3 shows the thickness dependence of the soft-mode frequency obtained from the fitting. The dashed line in the figure is the result of a linear fit to the data. Good correlation was observed between the soft-mode frequency and film thickness, and there was a tendency for the soft-mode frequency to decrease with decreasing film thickness. However, the *y*-intercept of the fit is approximately 1.6 THz, which is still much larger than the soft mode frequency of the STO film on the DSO substrate.

From the experimental results, it seems that not only the in-plane strain but also the *c*-axis length has a significant effect on the in-plane dielectric characteristics of STO films on MAO. The compressive in-plane strain in the film should induce an extension of the *c*-axis length in order to decrease the energy increased by the lattice deformation. This is implied by the lower-frequency shift of the soft-mode frequencies with a decrease in the film thickness as shown in **Table 1** and **Figure 2**. The longer extension of the *c*-axis in the STO films on MAO than that in the STO films on the other substrates might be induced by lattice defects such as oxygen and/or SrO vacancies [15], which may prevent the frequency shift of

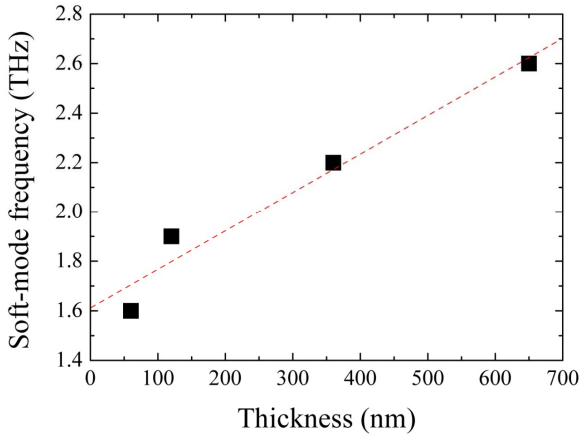

Figure 3. Thickness dependence of the soft-mode frequency of the $SrTiO_3$ thin films on $MgAl_2O_4$ substrates. The dashed line is a result of a linear fit.

Table 1. Lattice mismatch between $SrTiO_3$ and LSAT, $DyScO_3$, and $MgAl_2O_4$, thicknesses, and *c*-axis lengths of the STO films on each substrate.

Substrate	LSAT (100)	$DyScO_3$ (110)	$MgAl_2O_4$(100)		
Lattice mismatch	−0.95%	+0.99%	+3.39%		
Thickness (nm)	360	120	60	120	360, 650
c-axis length (nm)	0.3936	0.3885	0.3895	0.3899	0.3900

the soft mode and also an increase in the critical temperature T_c of STO thin films on MAO. Kim *et al.* [16] reported that extended *c*-axis lengths in STO films with constant in-plane lattice lengths changed the out-of-plane dielectric characteristics. Additionally, our study has implied that an extension of *c*-axis lengths also changes the in-plane dielectric characteristics of STO thin films.

4. Conclusion

STO thin films of different thicknesses were deposited on MAO, LSAT, and DSO substrates. The in-plane lattice constant of the 360 nm thick STO thin film on MAO was found to correspond to that of the MAO substrate, indicating that there was no relaxation of the in-plane strain in the film. The *c*-axis lengths of the STO film on MAO were determined to be longer due to in-plane compressive strain; however, the values were smaller than that expected from the trends observed in the other substrates. The soft-mode frequencies of the films shifted to lower frequencies with a decrease in the film thickness. The minimum soft-mode frequency of a STO thin film on MAO was found to be about 1.6 THz. These results indicate that the *c*-axis length of a STO thin film affects the in-plane dielectric characteristic of the STO film and that lattice defects prevent an increase in the T_c of the films.

5. Acknowledgements

The authors received technical support from T. Tanaka and T. Takehara for the X-RSM measurement. This study was supported by a Grant-in-Aid for Scientific Research (A) (No. 22246043) and the Core-to-Core Program of the Japan Society for the Promotion of Science (JSPS).

REFERENCES

[1] H. E. Weaver, "Dielectric Properties of Single Crystals of $SrTiO_3$ at Low Temperatures," *Journal of Physics and Chemistry of Solids*, Vol. 11, No. 3-4, 1959, pp. 274, IN5-IN6, 275-277.

[2] N. A. Pertsev, A. K. Tagantsev and N. Setter, "Phase Transitions and Strain-Induced Ferroelectricity in $SrTiO_3$ Epitaxial Thin Films," *Physical Review B*, Vol. 61, No. 2,

2000, pp. R825-R829. doi:10.1103/PhysRevB.61.R825

[3] J. H. Haeni, *et al.*, "Room-Temperature Ferroelectricity in Strained $SrTiO_3$," *Nature*, Vol. 430, No. 7001, 2004, pp. 758-761. doi:10.1038/nature02773

[4] G. Sheng, *et al.*, "A Modified Landau-Devonshire Thermodynamic Potential for Strontium Titanate," *Applied Physics Letters*, Vol. 96, No. 23, 2010, Article ID: 232902. doi:10.1063/1.3442915

[5] M. D. Biegalski, *et al.*, "Relaxor Ferroelectricity in Strained Epitaxial $SrTiO_3$ Thin Films on $DyScO_3$ Substrates," *Applied Physics Letters*, Vol. 88, No. 19, 2006, Article ID: 192907. doi:10.1063/1.2198088

[6] M. D. Biegalski, *et al.*, "Influence of Anisotropic Strain on the Dielectric and Ferroelectric Properties of $SrTiO_3$ Thin Films on $DyScO_3$ Substrates," *Physical Review B*, Vol. 79, No. 22, 2009, Article ID: 224117. doi:10.1103/PhysRevB.79.224117

[7] P. Kužel, C. Kadlec, F. Kadlec, J. Schubert and G. Panaitov, "Field-Induced Soft Mode Hardening in $SrTiO_3$/$DyScO_3$ Multilayers," *Applied Physics Letters*, Vol. 93, No. 5, 2008, Article ID: 052910. doi:10.1063/1.2967336

[8] D. Nuzhnyy, *et al.*, "Soft Mode Behavior in $SrTiO_3$/$DyScO_3$ Thin Films: Evidence of Ferroelectric and Antiferrodistortive Phase Transitions," *Applied Physics Letters*, Vol. 95, No. 23, 2009, Article ID: 232902. doi:10.1063/1.3271179

[9] P. Kužel, F. Kadlec, J. Petzelt, J. Schubert and G. Panaitov, "Highly Tunable $SrTiO_3$/$DyScO_3$ Heterostructures for Applications in the Terahertz Range," *Applied Physics Letters*, Vol. 91, No. 23, 2007, Article ID: 232911. doi:10.1063/1.2822409

[10] R. Kinjo, I. Kawayama, H. Murakami and M. Tonouchi, "Strain-Induced Ferroelectricity of a $SrTiO_3$ Thin Film on a $MgAl_2O_4$ Substrate Observed by Terahertz Time-Domain Spectroscopy," *Journal of Infrared Millimeter, and Terahertz Waves*, Vol. 33, No. 1, 2012, pp. 67-73. doi:10.1007/s10762-011-9839-9

[11] R. Kinjo, *et al.*, "Observation of Strain Effects of $SrTiO_3$ Thin Films by Terahertz Time-Domain Spectroscopy with a 4-Dimethylamino-*N*-methyl-4-stilbazolium Tosylate Emitter," *Japanese Journal of Applied Physics*, Vol. 48, No. 9, 2009, Article ID: 09KA16. doi:10.1143/JJAP.48.09KA16

[12] R. A. Cowley, "Temperature Dependence of a Transverse Optic Mode in Strontium Titanate," *Physical Review Letters*, Vol. 9, No. 4, 1962, pp. 159-161. doi:10.1103/PhysRevLett.9.159

[13] A. S. Barker, Jr. and M. Tinkham, "Far-Infrared Ferroelectric Vibration Mode in $SrTiO_3$," *Physical Review*, Vol. 125, No. 5, 1962, pp. 1527-1530. doi:10.1103/PhysRev.125.1527

[14] H. Vogt, "Refined Treatment of the Model of Linearly Coupled Anharmonic Oscillators and Its Application to the Temperature Dependence of the Zone-Center Soft-Mode Frequencies of $KTaO_3$ and $SrTiO_3$," *Physical Review B*, Vol. 51, No. 13, 1995, pp. 8046-8059. doi:10.1103/PhysRevB.51.8046

[15] C. H. Park and D. J. Chadi, "Microscopic Study of Oxygen-Vacancy Defects in Ferroelectric Perovskites," *Physical Review B*, Vol. 57, No. 22, 1998, pp. R13961-R13964.

[16] Y. S. Kim, *et al.*, "Observation of Room-Temperature Ferroelectricity in Tetragonal Strontium Titanate Thin Films on $SrTiO_3$ (001) Substrates," *Applied Physics Letters*, Vol. 91, No. 4, 2007, Article ID: 042908. doi:10.1063/1.2764437

